Properties of Crystalline and Amorphous Silicon Telluride*

Kurt E. Petersen, Ulrich Birkholz,† and David Adler

Department of Electrical Engineering and Center for Materials Science and Engineering, Massachusetts Institute of Technology, Cambridge, Massachusetts 02139

(Received 29 December 1972)

Single crystals of silicon telluride, which has an unusual 2:3 stoichiometry, have been grown by a chemical vapor deposition technique. A photoluminescence level at 1.3 eV has been found as well as strong EPR signals, suggesting defects in the crystal which also could explain other unusual features. Thin films and bulk samples of silicon telluride glasses, Si_xTe_{1-x}, $0.02 \leq x \leq 0.25$, were prepared and examined by optical absorption, photoconductivity, infrared transmission, electrical conductivity, Hall effect, differential thermal analysis, EPR, and x-ray experiments. The values of the energy gap (0.7 to 1.0 eV), resistivity ($\sim 5 \times 10^5$ Ω cm), and glass transition temperature (120 to 175 °C) were found to increase throughout the glass-forming region, with increasing silicon. Some microscopic structural features are shared by crystal and glass, including the presence of $SiTe_4$ tetrahedra, interatomic distances and reststrahlen absorption bands, even though the bonding seems to change from largely ionic in the crystal to largely covalent in the glasses. No EPR signal could be detected in the bulk glasses down to 77 °K. The Hall mobility of the glasses is approximately 1.0 cm^2/V sec, independent of room temperature from 200 to 300 °K, and indicates the predominance of hole conduction. No polaron effects are evident. Structurally, a covalent model consisting of tetravalent silicon and divalent tellurium is consistent with all the data for the amorphous system.

I. INTRODUCTION

Although most IV-VI crystals exist in 1:1 or 1:2 stoichiometries, crystalline silicon telluride belongs to a very small group with an unusual 2:3 stoichiometry. The only other known members of this group are Ge_2S_3,[1] Sn_2S_3,[2] and Sn_2Se_3.[3] All three of these binary systems also form crystals with the more common 1:1 and 1:2 ratios. On the other hand, Bailey has shown that Si_2Te_3 is the only crystal in the silicon-tellurium system.[4] Crystalline silicon telluride exhibits several other interesting electronic features, including a very low Hall mobility and thermal conductivity, a relatively high electrical resistivity, and a large optical band gap. These features alone make this crystal an interesting material to study. In the context of amorphous chalcogenides, however, which often show these same qualitative characteristics, the distinctions between such a chalcogenide crystal and its amorphous counterpart take on new significance. In addition, a study of amorphous silicon telluride adds to our knowledge of the simpler binary chalcogenide systems, many of which have recently been investigated extensively.

With these thoughts in mind, several new experiments were performed on crystalline silicon telluride and a preliminary investigation of the amorphous system Si_xTe_{1-x}, where $0.02 \leq x \leq 0.25$, was undertaken. This investigation centered on the compositional variation of the optical energy gap and some structural features in the two phases.

II. EXPERIMENTAL PROCEDURE

Samples of amorphous silicon telluride were prepared in both bulk and thin-film form. The majority of the thin-film samples reported on in this work were sputtered from a target of polycrystalline Si_2Te_3. Single crystals were grown by vapor transport in sealed quartz ampoules at about 750 °C, as explained elsewhere in the literature.[4-7] These crystals were ground in a dry N_2 atmosphere, pressed into a 1-in. diameter target 0.2–0.3 cm thick, and glued with silver epoxy onto an aluminum mount. The target was sputtered clean (i.e., a shutter held over the substrate) for 0.5 to 1.0 h before each deposition. All sputtering was done at 10–15-mTorr pressure of high-purity argon. Both source and substrate were water cooled. Slightly different sputtering conditions yielded different film compositions partly due to the relatively high vapor pressure of tellurium (0.1 mTorr) typical at source temperatures (280 °C), corresponding to sputtering power densities less than 3 W/cm^2.

Thin-film compositions varied from 2 to 25-at.% silicon as determined from chemical and electron-microprobe x-ray-fluorescence analysis. The amount of crystallinity in each sample was deduced from x-ray-diffraction patterns. No sharp x-ray structure was observed in the samples reported here, unless stated otherwise.

The silicon-tellurium system has a bulk-glass-forming region from approximately 15 to 25-at.% silicon. Several compositions of bulk glasses from this region were fabricated. Small chunks of tellurium and silicon were placed in quartz ampoules of various configurations, evacuated to about 10^{-6} Torr, and sealed. These ampoules were placed in a furnace at temperatures above the liquidus and quenched in either air or water.

Unlike crystalline Si_2Te_3, the amorphous mate-

rial seems to have negligible decomposition in air and some bulk samples were even machined and polished using water as a coolant. Nevertheless, all samples were stored in vacuum except during the experiments. Annealing cycles were performed either in vacuum or in an argon atmosphere.

A Keithley electrometer with an input impedance of 10^{14} Ω was used in resistance measurements. For our optical data, Beckman IR-12 infrared and Cary model-14 spectrophotometers were used. Plots of the derivative of the heat capacity with respect to temperature (DTA) were obtained from a Perkin–Elmer differential scanning calorimeter.

III. CRYSTALLINE SILICON TELLURIDE

Very little is known about IV-VI compounds of 2:3 stoichiometry, although silicon telluride has been the most studied of these materials. Three factors have made this crystal difficult to investigate and uninteresting as a device material. It is very hygroscopic, and the deep red crystal quickly turns black upon exposure to ordinary air through a reaction such as

$$Si_2Te_3 + 4H_2O \rightarrow 2SiO_2 + 2H_2Te + Te + 2H_2.$$

The SiO_2 and free tellurium have been identified on the surface of decomposed crystals[5] (the black appearance being due to Te) and H_2Te is readily recognized by its strong odor.

Second, silicon telluride has an unfortunate doping behavior. It appears to be a highly compensated semiconductor which shows p-type conduction over a wide range of dopants and whose resistivity generally increases with relatively large concentrations of impurities.[4]

Third, the Si_2Te_3 crystal structure seems to be inherently defective. This high defect density accounts for the very low thermal conductivity, 1–5 mW/°C cm,[4,8] and very low mobility, < 1 cm^2/V sec,[4] as well as several other unusual characteristics.

For many years, it was thought that silicon telluride crystallizes with a 1:2 stoichiometry. Weiss and Weiss[9] used this assumption in the interpretation of their x-ray data and suggested a CdI_2 structure, in which the Te atoms form a hexagonal close-packed array and the Si atoms occupy the octahedral interstices between alternate Te layers. The Si-Te distance in this structure would be 3.04 Å.[9] However, after detailed measurements, Hanevald *et al.*[6] confirmed the hcp tellurium arrangement, but tentatively concluded that $\frac{3}{4}$ of the silicon atoms occupy *tetrahedral* interstices, with only $\frac{1}{4}$ in octahedral interstices. This structure yields a nearest-neighbor Si-Te distance of 2.62 Å. The present model for Si_2Te_3 is that $\frac{3}{4}$ of the Si atoms occupy tetrahedral interstices between *alternate* Te layers, while the remaining $\frac{1}{4}$ occupy octahedral interstices between the remaining Te layers. In this case, the Si-Te distance for octahedral Te is 2.84 Å. Because of the nonideality of the hcp Te array, the Te-Te separations vary from 4.01 to 4.33 Å. Half of the Te atoms are fourfold coordinated and half are twofold coordinated. This fact, together with the highly hygroscopic nature of the material, implies a strong ionic component to the Si_2Te_3 crystal.

The phase diagram for the Si-Te system has been determined by Bailey, whose investigations also showed Si_2Te_3 to be the only crystalline compound in this system. Bailey and others[10,11] have prepared glasses in the region from 15- to 25-at.% silicon. The amorphous samples that we have studied have compositions generally within this region. Other thermodynamic properties of the Si-Te system have been studied by Brebrick[10] and Exsteen *et al.*[7]

Most of what is presently known about the electronic structure of Si_2Te_3 comes from optical measurements. The quality of the data is limited partly by the rapid rate of decomposition of the surface. Nevertheless, Rau and Kannewurf[5] deduced three transitions from their optical-absorption data. Weak indirect forbidden and indirect allowed transitions occur at 1.82 and 1.89 eV, respectively. A forbidden direct edge at 2.18 eV, which accounts for most of the absorption spectrum, also gives rise to a sharp photoconductivity peak at the same energy. We have found a blue shift in the absorption edge of about 1.0 meV/°K down to 77 °K and also a very interesting photoluminescence level (see Fig. 1). This level is about 0.3 eV wide and is centered at 1.3 eV. It is believed to be due to crystal defects, which could also account for the low mobility and low thermal conductivity of Si_2Te_3. We have observed large orientation-dependent EPR signals at room temperature in the crystal, further evidence for these same defects or vacancies.

Infrared-transmission data normal to the c axis of the crystal are shown in Fig. 2. The first three peaks, at 13.8, 20.2, and 23.2 μ, are due to TeO_2, some of which forms on the surface. The other peak, at 32 μ, is most likely a reststrahlen band whose amplitude is affected by both orientation and the amount of ionicity in the bonding.

Data on the electrical properties of Si_2Te_3 are even more scant. Smirous *et al.*[12] and Bailey[4] have measured resistivity as a function of temperature on polycrystalline samples with at least qualitatively similar results. Just above room temperature, polycrystalline samples exhibit an activation energy of 0.1–0.2 eV. Below 300 °K, this energy is reduced to about 0.05 eV. Polycrystalline conductivity at room temperature is about 10^{-3} Ω^{-1} cm^{-1}, is p type, and decreases when doped

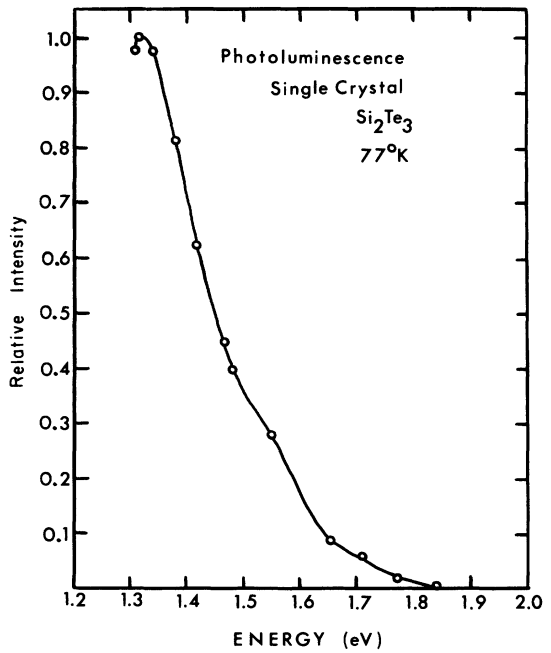

FIG. 1. Photoluminescence level in the gap of crystalline Si_2Te_3.

with Si, Te, Cu, Mn, Fe, As, Cd, and Ga.[4] When measured along the c axis, however, a value of $10^{-9}\ \Omega^{-1}\ cm^{-1}$ was found by Rau and Kannewurf.

Bailey noticed a sharp, reversible decrease in conductivity and increase in Seebeck coefficient near 400 °C and attributed this to a structural change in the crystal. On the other hand, differential-thermal-analysis data on single-crystal Si_2Te_3 reported here show no change in heat capacity at or near 400 °C. The exact nature of this transition, if one actually exists, thus remains unknown.

In summary, crystalline silicon telluride is partially ionic, and forms a very complex hexagonal lattice. The exact reason for the 2:3 stoichiometry is still unknown, although there are a few other IV-VI compounds with this stoichiometry. The ir spectrum shows evidence of a TeO_2 impurity band as well as a Si-Te reststrahlen band.

Single crystals exhibit a low mobility, low thermal conductivity, low electrical conductivity, and a highly compensated electronic character, all indicating a defective lattice. A strong, broad photoluminescence level and EPR signal substantiate the evidence for these defects. The band gap is large and indirect, although the electrical activation energy, being defect controlled, is very low.

IV. PROPERTIES OF AMORPHOUS SILICON TELLURIDE

A. Optical Properties

Absorption spectra in the range from 2.5 μ (0.5 eV) to 0.2 μ (6.2 eV) were taken for both bulk and thin-film samples. Typical thin-film samples were 2000 Å to 5 μ thick on quartz or glass substrates. Many exhibited the well-known interference patterns in the region of low absorption. After determining the thickness d from a Zeiss double-beam interferometer, the index of refraction could be determined from the formula

$$n = \frac{N\lambda_i\lambda_j}{2d(\lambda_i - \lambda_j)} ,$$

where N is the number of maxima between λ_i and λ_j. The results were in good agreement with those calculated from the reflection data of Hilton *et al.*[13] by means of the usual expression

$$R = \frac{(n-1)^2}{(n+1)^2} .$$

Amorphous $Si_{20}Te_{80}$ has an index of refraction $n = 3.4$ at a wavelength of 2 μ. Absorption measurements were also performed on three samples of bulk amorphous glasses with compositions of 15-, 20-, and 25-at.% Si. These samples were melted into very thin quartz ampoules, and were never exposed to air. The shapes of the absorption-coefficient curves for the thin films were similar to the bulk samples. The magnitude of the absorption coefficient of the glasses, however, was lower than that of the thin film by two orders of magnitude. This last result, although commonly observed in other materials, is not yet understood.

Although the absorption edge of sputtered thin films did decrease initially upon annealing, such effects were absent in bulk vacuum-sealed samples, as indicated in Fig. 3. This sample was annealed five times (approximately one hour each time) at steadily increasing temperatures; no change in optical absorption was observed until the crystallization temperature was reached. X-ray analysis of this sample after the final anneal showed

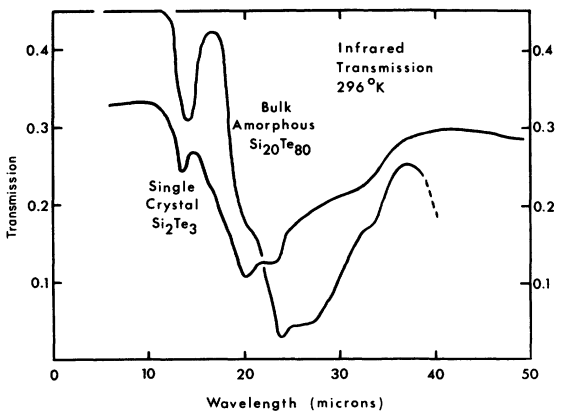

FIG. 2. Infrared transmission at room temperature for crystalline Si_2Te_3 (normal to c axis) and bulk amorphous $Si_{20}Te_{80}$.

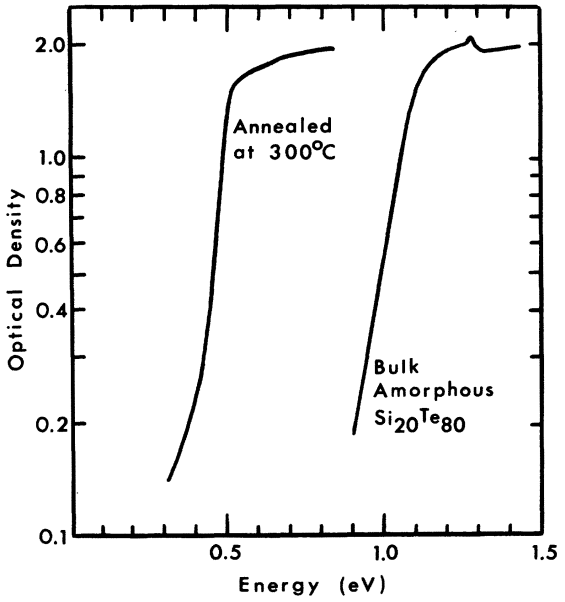

FIG. 3. Effect of annealing bulk amorphous $Si_{20}Te_{80}$ above the crystallization temperature. The annealed sample had a band gap close to that of crystalline tellurium and, when x rayed, showed lines of both crystalline tellurium and crystalline Si_2Te_3.

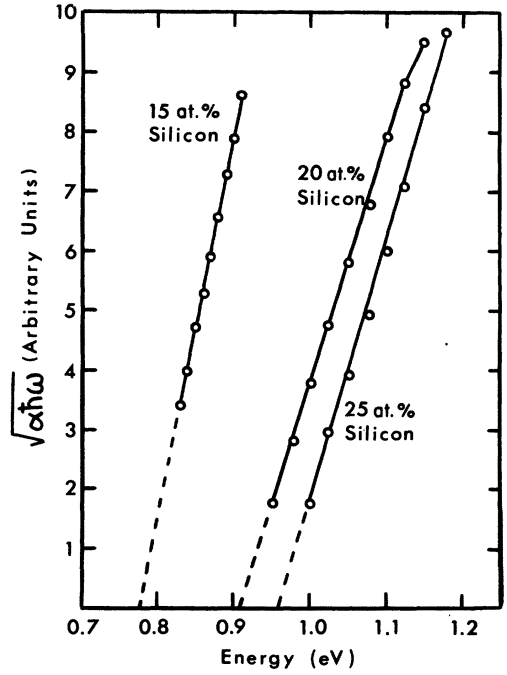

FIG. 4. Plots of $(\alpha\hbar\omega)^{1/2}$ vs $\hbar\omega$ for three bulk amorphous samples of different silicon concentrations. E_{opt} corresponds to the extrapolation of the straight-line segments to the energy axis.

lines from both crystalline Te and crystalline Si_2Te_3, indicating phase separation and crystallization had occurred. E_{opt}, the optical gap, for all amorphous samples was determined from plots of $(\alpha\hbar\omega)^{1/2}$ vs $\hbar\omega$. This method has been suggested by Tauc[14] and by Mott[15] for amorphous semiconductors, for which k conservation is not an important selection rule. The intercept of the straight-line section of such plots with the energy axis gives E_{opt}, as indicated in Fig. 4.

An interesting aspect of the optical data is the variation of E_{opt} with composition, shown in Fig. 5. The minimum in E_{opt} at 12–14-at.% Si appears to be a real effect. This point corresponds to the eutectic composition in the silicon-tellurium-system phase diagram. In fact, the entire graph of E_{opt} vs at.% Si seems to follow the general characteristics of the phase diagram. Note that partial crystallization often occurred below 5-at.% silicon, as we would expect from the very low crystallization temperature of tellurium, ~10 °C.[16] The energy gap of these crystallized samples is less than that of the corresponding amorphous materials.

Photoconductivity was measured in only one sample, bulk amorphous $Si_{20}Te_{80}$, at 120 and at 300 °K. Electrons per incident photon vs energy is shown in Fig. 6 at 300 °K. The shape of the photoresponse curve is similar to that of the actual absorption coefficient. In fact, at both temperatures, plots of $(\eta\hbar\omega)^{1/2}$ vs energy (where η = electrons/in-

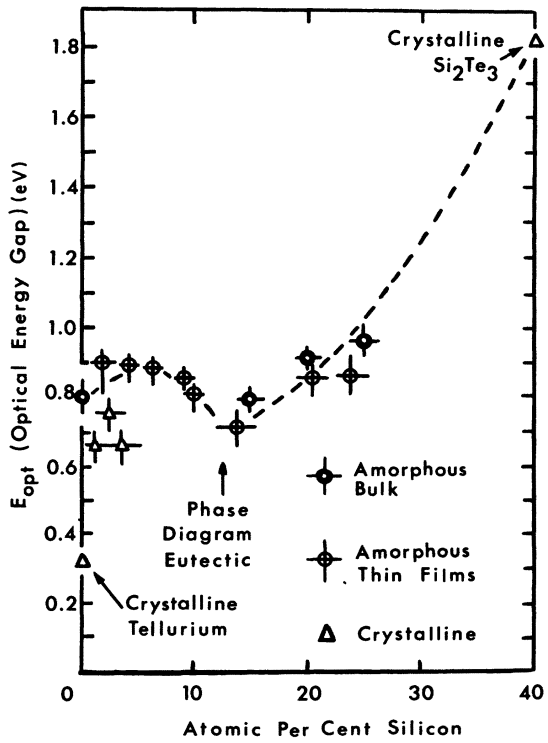

FIG. 5. Optical energy gap vs composition for various amorphous and crystalline samples.

cident photon) are linear and extrapolate to $E(\eta) = 0.84$ at 300 °K and $E(\eta) = 0.99$ at 120 °K. These values yield the temperature variation of the photoconductivity energy gap $E_g(\eta)$. Measurements of E_{opt} were also done at the two temperatures. We found

$$\frac{dE_g(\eta)}{dT} = -0.8 \text{ meV/°K},$$

$$\frac{dE_{opt}}{dT} = -0.6 \text{ meV/°K},$$

which compare well with the value of -0.7 meV/°K found by Fagen *et al.*[17] for amorphous $Si_{20}Te_{80}$.

Although the region of overlapping absorption and photoconductivity data is small, a plot of quantum efficiency (η/α) as a function of energy indicates that the quantum efficiency decreases slowly between 0.9 and 1.1 eV and levels off near 1.1 eV. A similar behavior was also observed by Fagen and Fritzsche[18] in a multicomponent chalcogenide glass.

B. Electrical Properties

Several types of resistance-vs-temperature measurements were performed on both bulk and thin-film samples. A plot of $\ln\rho$ vs $1/kT$ is shown in Fig. 7. Four-point Van der Pauw techniques were used above room temperature, and a two-point probe measurement was done above and below room temperature. The two-point data are consistent with the four-point results, thus indicating a negligible contact resistance. The resistivity obeys the usual semiconductor relation, $\rho = \rho_0 e^{E_A/kT}$ with activation energy E_A varying from about 0.55 eV at 400 °K to 0.44 eV at 200 °K for $Si_{20}Te_{80}$. Sandwich-type thin-film structures yield comparable values for E_A below room temperature, where most of these measurements were performed. In all these samples, bulk and thin-film, the activation energy decreased sharply below 220 °K, as shown in the figure.

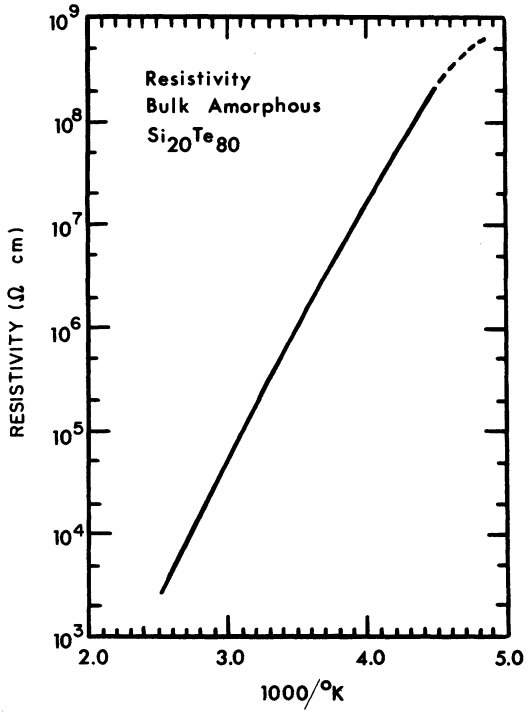

FIG. 7. Electrical resistivity vs inverse temperature for amorphous $Si_{20}Te_{80}$. The activation energy varies from 0.55 to about 0.44 eV at 400 and 200 °K, respectively.

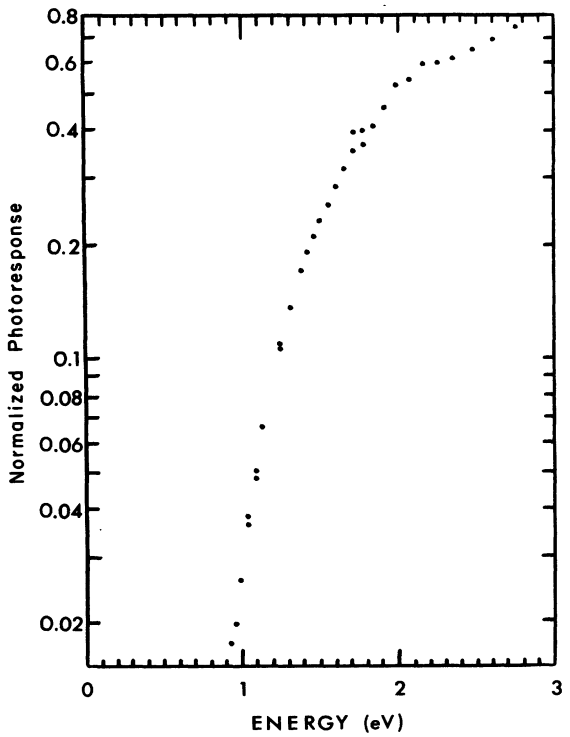

FIG. 6. Normalized photoresponse (electrons per incident photon) at room temperature.

The room-temperature resistivities and the high-temperature (50–100 °C) activation energies for three bulk-glass compositions are shown in Figs. 8 and 9. The resistivity behaves more or less as would be expected; tellurium has a much lower resistivity than silicon telluride. The activation energies for 15- and 20-at.% silicon follow the behavior of E_{opt} vs composition, also as might be expected. The point given for 25-at.% silicon, however, is somewhat surprising. Further comparison of E_{opt} and E_A reveals that $2E_A > E_{opt}$ for the 15- and 20-at.% samples, but not for the 25-at.% silicon sample.

Hot-point probe measurements on bulk glasses indicate conduction is dominated by holes, just as in the crystal. This is in agreement with Hall

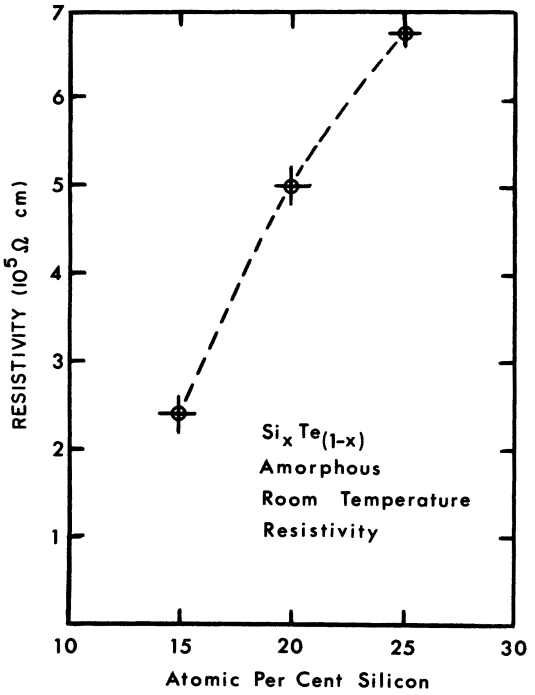

FIG. 8. Room-temperature resistance vs composition for bulk amorphous samples.

data, which yield a temperature-independent mobility near 1.0 cm^2/V sec between 200 and 300 °K.

Finally, nonlinear *I-V* characteristics of thin films were also noted by Altunyan *et al.*[11] They switched films of compositions near $Si_{20}Te_{80}$ in a memory mode, but the devices crystallized easily and operated only for a few cycles, owing presumably to phase separation into Te-rich and Si_2Te_3-rich regions. We also succeeded in memory switching both bulk and thin-film samples, but no characterization of switching parameters was attempted.

C. Structure

Information about the microscopic structure of silicon-tellurium glasses is based on data from several sources. We have performed chemical analysis, infrared transmission, differential thermal analysis, and electron paramagnetic resonance experiments. X-ray radial distribution studies have been carried out by Hilton *et al.*[13] as well as by Bartsch and Just.[19] Hilton *et al.*[13] have also reported some infrared data.

Unlike the crystal, silicon-tellurium glasses seem to be chemically very stable in air. No decomposition was noted in the bulk samples, although some thin films gave off the characteristic odor of H_2Te immediately after deposition. Bulk samples, in fact, were even machined and cleaned in water with no noticeable deterioration. This difference suggests that the glass is more covalently bonded than the crystal.

The infrared transmission spectrum of the glass is compared to that of the crystal in Fig. 2. The absorption peaks in the amorphous sample at 14.2 and 23.8 μ, as well as the shoulder at 20.3 μ, are due to TeO_2, the oxygen in this case probably originating as an impurity during sample preparation.[20] The small (~ 0.5 μ) upward shift of this TeO_2 spectrum and the differences in relative peak amplitude (particularly the peak near 20 μ) in going from the crystal to the glass are very likely due to the different environments of the TeO_2 in the two materials.

The absorption near 32 μ in the glass was also observed by Hilton *et al.*[13] and identified as a Si-Te vibrational mode. The fact that this absorption is also present in the crystal provides strong evidence of some similarities in short-range order between the two phases.

Two other bands are observed in the amorphous material. The absorption peak near 27 μ can be tentatively identified as a Te-Te vibrational mode, expected from the excess Te present in $Si_{20}Te_{80}$. A possible explanation of the absorption that sets in near 40 μ is excitation of acoustic phonon modes, active because of the breakdown of the k-conservation selection rule in the glass.

Measurements on bulk samples of 15-, 20-, and 25-at. % silicon showed no EPR signal down to liquid-nitrogen temperature. This is not conclusive evidence against the existence of unpaired spins, since it may only be that the relaxation times in the material are too rapid even at 77 °K (and, in fact, this

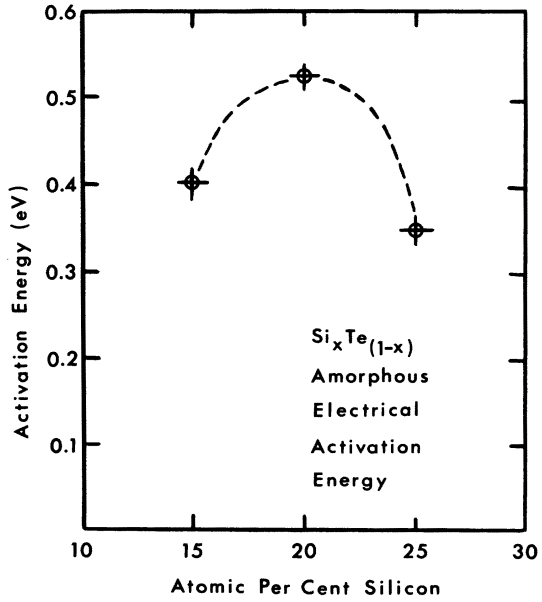

FIG. 9. Electrical activation energy (50 to 100 °C) vs composition for bulk amorphous samples.

may generally be the case in amorphous materials), but it does give support to the applicability of a covalent-bonding model to silicon-tellurium glasses, especially when contrasted with the large EPR signal found in crystalline Si_2Te_3, a defective and partially ionic structure.

We observed the three common glass phase transitions in the DTA for three bulk samples. The crystallization and melting points obtained are very close to those published by Altunyan *et al.*[11] The glass transition points are new data, however, and yield an interesting plot as a function of composition, shown in Fig. 10. This trend of increasing T_g with increasing silicon concentration is similar to the plots of E_{opt} and resistivity vs composition (Figs. 5 and 8) throughout the glass-forming region, and is readily understandable. Tellurium tends to be soft and silicon tends to be hard; so the behavior of the softening temperature is as we would expect. In fact, the extrapolation of the curve shown in Fig. 10 is extremely suggestive of continuous behavior throughout the Si_2Te_3-Te system, in that the value extrapolated to 40-at.% silicon is actually the crystallization temperature of Si_2Te_3, while that extrapolated to pure Te is indeed the crystallization temperature of Te(10°C). A further conclusion which can be inferred from the sharp increase of T_g with increasing Si concentration evident in Fig. 10 is that it is unlikely that the Si-Te system phase separates.

Another interesting aspect of the Si-Te system is that the nearest-neighbor tetrahedral Si-Te distance (2.62 Å) in the crystal is very close to the sum of the atomic radii of tetravalent Si (1.17 Å) and divalent Te (1.43 Å). Such a nearest-neighbor separation can also be expected in the glass, according to the small-x model of Betts *et al.*[21] In addition, Bartsch and Just,[19] in their x-ray radial distribution analysis on amorphous $Si_{19}Te_{81}$, found that their data are best explained by a tetrahedral configuration of $SiTe_4$ with divalent Te and tetravalent Si. Furthermore, their first-neighbor peak at 2.78 Å is consistent with the weighted average of the Si-Te and Te-Te bond distances. Since Te is a much stronger x-ray scatterer than Si, a substantial shift toward the Te-Te distance (2.86 Å) can be expected. Hilton *et al.*[13] found a much smaller first-neighbor distance (2.62 Å), exactly the tetrahedral Si-Te distance in the crystal. However, their data exhibit large termination errors, as indicated by significant structure in the radial distribution function below 2 Å. If the nearest-neighbor Si-Te distance in the glass is indeed near 2.62 Å, then it can be concluded that the $SiTe_4$ tetrahedra remain substantially intact in the amorphous phase, despite a change to more covalent bonding relative to that of the crystal. This may also account for the previously discussed similarities in the infrared-transmission spectra.

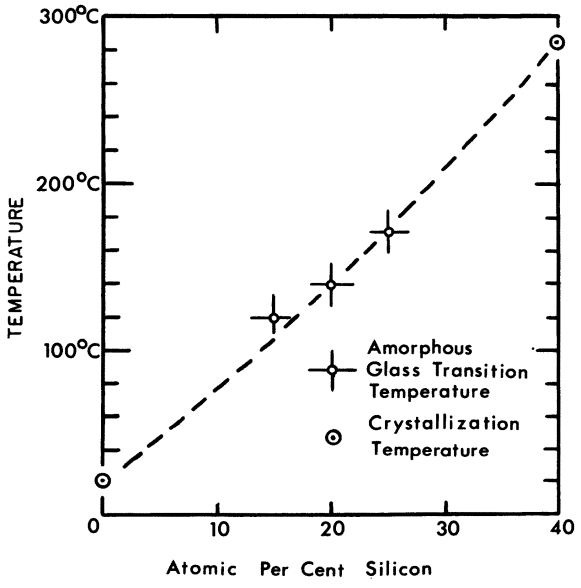

FIG. 10. Glass transition temperatures for bulk amorphous silicon telluride samples and crystallization temperatures for Si_2Te_3 and Te.

In summary, the following can be concluded about the structure of Si-Te glasses from a combination of the previous work[13,19] and the results presented here: (i) Si-Te bonds form in preference to Te-Te or Si-Si bonds; (ii) nearest-neighbor Si-Te separations are similar to those found in crystalline Si_2Te_3; (iii) the bonding is primarily covalent, involving tetravalent Si and divalent Te; (iv) the glasses exhibit fewer dangling-bond-type defects than the crystal, consistent with their amorphous covalent nature.

V. DISCUSSION

We have tried to emphasize in the discussion on the properties of these glasses that many of their characteristics, particularly structure, ir spectrum, glass transition temperature, optical energy gap, and resistivity, can be inferred, or at least are not unexpected, from what we already know about elemental silicon and tellurium, and crystalline silicon telluride. This very general predictability is one important aspect of this system.

Although the optical energy gap E_{opt} within the bulk-glass-forming region increases with increasing Si concentration in a manner similar to the room-temperature resistivity and the glass transition temperature, the additional data points available from Fig. 5 below 15-at.% Si indicate a variation that can be correlated with the Si-Te phase diagram. It appears that the energy gap of the glass is strongly related to its cohesive energy, even to the extent that a minimum in the gap occurs

near the eutectic composition.

The photoconductivity spectrum is generally parallel to that of the optical absorption coefficient, as is often the case in amorphous materials. Furthermore, the variation of the optical gap with temperature exhibits a typical slow decrease with increasing temperature. The electrical activation energy is larger than half the optical gap in two of the three glasses investigated, but not for the 25-at.% Si sample, which does not seem to follow all the other trends. The room-temperature resistivity, however, does monotonically increase with increasing Si over the compositional range investigated. The mobility is essentially independent of temperature, so that small-polaron effects do not appear to be important in these glasses. Conduction is predominatly p type, and even the Hall coefficient is positive.

We feel that some of the most important results of this study are the structural implications. Microscopically, both the crystal and the glasses, while differing in the amount of ionicity in their bonds, appear to cling to a basic tetrahedral arrangement. In the crystal, which is partially ionic, the silicon atoms probably occupy mostly tetrahedral interstices. In the glasses, the silicon atoms seem to maintain their tetrahedral positions with respect to the tellurium atoms, while the bonds become more covalent. However, the nearest-neighbor tetrahedral distances remain about the same in the two phases, at least when contrasted with the very different interatomic separations in crystalline and amorphous GeTe.[21,22]

Reflecting these structural similarities, the infrared transmission spectra of the two phases of silicon telluride are very similar, except for the additional long-wavelength absorption in the glass. Macroscopically, a larger Te content softens the structure, as evidenced by the decrease in T_g with decreasing Si concentration. This result also indicates the absence of phase separation in the system. Finally, the lack of an EPR signal in the glasses taken together with its strong presence in the crystal suggests that the amorphous material has much fewer dangling bonds, another indication of a covalent structure with local fulfillment of all valence requirements.

The similarities in microscopic structure between the amorphous and crystalline phases is the feature which gives rise to the predictability (by interpolation) of many of the properties of the silicon-tellurium system. This connection between short-range order and the properties of a solid is at the foundation of present-day amorphous theory. It has been observed in many materials, including silicon, germanium, As_2Se_3 (see Ref. 23 for a detailed review), that many of the fundamental characteristics of a material do not change drastically in going from crystalline to amorphous, provided the short-range order does not change. On the other hand, there are large differences between, for example, crystalline and amorphous GeTe,[21,22] whose short-range order is different in the two phases.

Although the amorphous silicon-tellurium glasses seem now to be very typical of other amorphous materials, there is still much to be learned about and from the silicon-tellurium system. Its real interest lies primarily in contrast and comparison with the crystal. In a certain sense, the amorphous state of this material seems to be more orderly and predictable than the crystal. A particularly revealing experiment would be mobility vs composition. Although it is likely that the extremely low observed mobility of crystalline Si_2Te_3 is primarily due to the highly defective lattice, it is interesting that this is a system in which the mobility in the crystalline phase is of the same order of magnitude as the mobility in the amorphous phase, a very unusual circumstance. Thus, the silicon-tellurium system provides a special opportunity to investigate purely the effects of long-range disorder on a given class of materials, without any other major concomitant changes.

ACKNOWLEDGMENTS

The authors would like to thank Floyd Arntz, Bimal Mathur, Donnie Reinhard, Anthony Colozzi, Michael Rechtin, Janis Kalnajs, Claire Schlenker, Tom Davis, and many others at the M. I. T. Center for Materials Science and Engineering for their aid and advice in the experimental work.

---

*Research supported by the Advanced Research Projects Agency of the Department of Defense and monitored by the U. S. Army Research Office, Durham, under Contract No. DAHC-04-70-C-0048.

†Now at the Institut für Angewandte Physik, Universität Karlsruhe, German Federal Republic.

[1]H. Spandau and F. Klanberg, Z. Anorg. Allg. Chem. **295**, 291 (1958).
[2]D. Mootz and R. Kunzman, Acta Crystallogr. **15**, 913 (1962).
[3]L. Polatnik and V. Levitin, Dokl. Akad. Nauk SSSR **96**, 975 (1955).
[4]L. G. Bailey, J. Phys. Chem. Solids **27**, 1593 (1966).
[5]J. W. Rau and C. R. Kannewurf, J. Phys. Chem. Solids **27**, 1097 (1966).
[6]A. J. K. Hanevald, W. Van der Veer, and F. Jellinek, Recl. Trav. Chim. Pays-Bas **87**, 255 (1968).
[7]G. Exsteen, J. Drowart, A. Van der Auwera-Mahieu, and R. Callaerts, J. Phys. Chem. 71, 4130 (1967).
[8]J. Vennik and R. Callaerts, C. R. Acad. Sci. (Paris) **260**, 496 (1965).
[9]A. Weiss and A. Weiss, Z. Anorg. Allg. Chem. **273**, 124 (1953).
[10]R. F. Brebrick, J. Chem. Phys. **49**, 2584 (1968).

[11]S. A. Altunyan, V. S. Minaev, M. S. Minazhdinov, and B. K. Skachkov, Fiz. Tekh. Poluprovodn. 4, 2214 (1970) [Sov. Phys.-Semicond. 4, 1906 (1971)].
[12]K. Smirous, L. Stourac, and J. Bednar, Czech. J. Phys. 7, 120 (1957).
[13]A. R. Hilton, C. E. Jones, R. D. Dobrott, H. M. Klein, A. M. Bryant, and T. D. George, Phys. Chem. Glasses 7, 116 (1966).
[14]J. Tauc, in *Optical Properties of Solids*, edited by F. Abeles (North-Holland, Amsterdam, 1969), p. 123.
[15]N. F. Mott, Philos. Mag. 19, 835 (1969).
[16]J. Stuke, J. Non-Cryst. Solids 4, 1 (1970).
[17]E. A. Fagen, S. H. Holmberg, R. W. Seguin, J. C. Thompson, and H. Fritzsche, in *Proceedings of the Tenth International Conference on the Physics of Semiconductors, Cambridge, Mass., 1970*, edited by S. P. Keller, J. C. Hensel, and F. Stern (U.S. Div. Tech. Inform., Oak Ridge, Tenn., 1970) p. 672.
[18]E. A. Fagen and H. Fritzsche, J. Non-Cryst. Solids 2, 180 (1970).
[19]G. Bartsch and T. Just, Z. Metallkd. 63, 360 (1972).
[20]A. R. Hilton and C. E. Jones, Phys. Chem. Glasses 7, 112 (1966).
[21]F. Betts, A. Bienenstock, and S. R. Ovshinsky, J. Non-Cryst. Solids 4, 554 (1970).
[22]D. B. Dove, M. B. Heritage, K. L. Chopra, and S. K. Bahl, Appl. Phys. Lett. 16, 138 (1970).
[23]D. Adler, Crit. Rev. Solid State Sci. 2, 317 (1971).

PHYSICAL REVIEW B VOLUME 8, NUMBER 4 15 AUGUST 1973

Microwave Magnetic Dipole Interaction in Small InSb Spheres: Induced Cyclotron-Resonance-Like Absorption in the Rayleigh Limit*

Thomas A. Evans[†‡] and Jacek K. Furdyna
Department of Physics, Purdue University, West Lafayette, Indiana 47907
(Received 10 October 1972; revised manuscript received 30 March 1973)

We report a new type of microwave resonant absorption observed in small spheres of n-type InSb at 35 GHz and 77 °K. The resonance is excited by the time-varying *magnetic* field, and occurs at approximately three times the cyclotron-resonance frequency. Although an exact theory for the phenomenon does not exist, the effect is examined in terms of an approximate analysis. It is formally identified as the magnetic dipole mode of oscillation of a bounded free-carrier plasma.

I. INTRODUCTION

Conventional microwave studies of cyclotron resonance in semiconductors are carried out on small specimens located in a resonant cavity, usually at the position of maximum microwave electric field E_{rf}. These experiments are restricted to very pure specimens, with carrier concentration N typically below 10^{13} cm^{-3}. The reason for this restriction is that when N is large, resonant absorption by the sample as a whole is shifted away from the cyclotron-resonant condition because of depolarizing effects,[1] and the experiment is no longer useful as a measure of the effective mass. Since the magnitude of the shift is determined by the plasma frequency $\omega_p \equiv (Ne^2/m^*\epsilon_l)^{1/2}$ of the free-carrier system (where m^* is the effective mass and $\epsilon_l = \epsilon_0 K_l$ is the lattice permittivity), the effect is often referred to as "magnetoplasma" shift.

The depolarizing effects are a consequence of the existence of fields (and therefore also currents) normal to the surface of the sample, which lead to accumulation of "polarization" charge at the boundaries. If we could eliminate the component of the current directed into the sample surface, the magnetoplasma shift of cyclotron resonance should automatically vanish.

Such situation is, in principle, possible when a spherical particle is selectively excited by a time-varying magnetic field, H_{rf}: the electric field induced by H_{rf} is purely solenoidal, and the currents excited in the (isotropic) particle are therefore everywhere transverse to the sample radius. This field configuration is depicted in Fig. 1 for the case of an isotropic sphere which is smaller than the spatial variation of H_{rf} inside as well as outside of the sample (the Rayleigh limit).

In practice, separate excitation by H_{rf} can be realized in a microwave cavity by positioning the specimen at an electric field node (magnetic field antinode), e.g., at location B in Fig. 2. We would expect depolarizing effects to disappear in this situation. It should then be possible to extend cyclotron-resonance measurements to materials which are inaccessible to such studies because of magnetoplasma shift in the conventional experiment.[2,3]

With this in mind, we examine both theoretically and experimentally the response of a small semiconductor sphere at the magnetic field maximum in a microwave cavity. Since an exact analysis of the interaction of an electromagnetic wave with a *gyrotropic* sphere of arbitrary size is an unsolved problem in classical electrodynamics, we offer an approximate and intuitive treatment. Experimen-